HYDRODYNAMIC CHARACTERISATION OF A WET SCRUBBER FOR DIFFERENT FLOW REGIMES RELEVANT FOR POOL SCRUBBING AND FCVS

P. Papadopoulos[1,2], S.Tietze[1], D. Suckow[1], S.J. Ceder[1], B. Roth[1] and T. Lind[1]
[1]: Paul Scherrer Institut, 5232 Villingen, Switzerland
[2]: ETH Zürich, 8092 Zürich, Switzerland
sabrina.tietze@psi.ch
petros.papadopoulos@psi.ch
detlef.suckow@psi.ch
terttaliisa.lind@psi.ch

ABSTRACT

The mitigation of radioactivity during a severe accident in a nuclear power plant (NPP) is a key element in the accident management guidelines of any plant. Among the different radioactive substances originating from the damaged core, iodine is one of the most important volatile, radiotoxic elements that is potentially released into the environment. Modern NPPs provide safety measures to retain such contaminants and to therefore reduce radioactive emissions, e.g. with suppression pools in BWRs or filtered containment venting systems (FCVS). For FCVS that are based on wet scrubbers, and suppression pools, the retention of the different contaminants depends on multiple parameters, such as the chemical composition of the pools and the hydrodynamic characteristics.

In this work, the mid-scale facility ISOLDE at PSI was used for the investigation of the different realistic flow regimes that are established inside the pool in pure water for further studies on the retention of elemental iodine. ISOLDE was built as a sister unit of mini-VEFITA where iodine tests are performed under commercial chemical compositions. In the ISOLDE test facility, the bubble size distribution and interfacial area concentration were determined using a three-layer wire-mesh sensor. The acquired data and results match the results from literature and highlight once more the importance of understanding the bubble characteristics in pool scrubbers to improve the understanding of the mass transfer phenomenon.

KEYWORDS
Volatile Source Term, Filtered Containment Venting, Pool Scrubbing, Bubble Hydrodynamics, Two-Phase Flow Regime

1. INTRODUCTION

The safe and economic operation of a nuclear power plant (NPP) has a high priority for the utility operators. To assure this operation, safety measures have to be in place for the management of different accident scenarios. Among all these scenarios, severe accidents with fuel damage and release of activity into the containment or the environment are the most challenging ones. In this sense, Filtered Containment Venting Systems (FCVS) have come back into focus after the Fukushima accident [1] to protect the last barrier, the containment, from integrity failure due to overpressure and the release of the radioactive source term. The designs of current filters are based either on dry filters or wet scrubbers or even sequential combinations of both. In case of wet scrubbers, the efficiency for scrubbing contaminants from the gas stream is depending, among other various parameters, on the hydrodynamic properties of the flow.

The removal of gas phase iodine species has so far not been an easy task for wet scrubbers which lately lead to more thorough studies. Those studies tried to link different quantities like gas injection velocity, bubble residence time and iodine concentration in the gas stream or gas temperature with the removal efficiency of iodine using venturi geometries as gas inlet nozzles as presented in [2-6]. The studies agree that a higher gas injection flow rate in the venturi nozzle leads to higher iodine retention as long as the critical velocity is not exceeded. Same is true for a higher iodine concentration in the gas stream and a higher residence time in the pool which corresponds to a higher submergence of the inlet nozzle.
In previous studies at PSI using the mini-VEFITA test facility, a commercial injector nozzle that is not based on a venturi geometry was used to investigate the effects of submergence, residence time and iodine concentration on the decontamination factor (DF) with commercial chemical solutions [7]. In Figure 1, a schematic cut view of the full-scale filter is illustrated for the used geometry. The experiments in [7] were carried out with a reduced scale. This kind of FCVS is acting in three stages on the incoming gas stream. The first stage is the injection nozzle where the gas stream is broken up into smaller bubbles. In this area, most of the aerosols in the decontaminated gas stream are retained due to inertial effects and the turbulent injection condition. Part of the contaminants in the gas are also scrubbed already at this stage. The gas jet is in an additional step forced through multiple impactor plates above the nozzle and a Sulzer Chemtech mixing element to drive the bubble breakup inside the pool. At the top of the FCVS, a droplet separator makes sure that no contaminated liquid is exiting the filter into the environment.

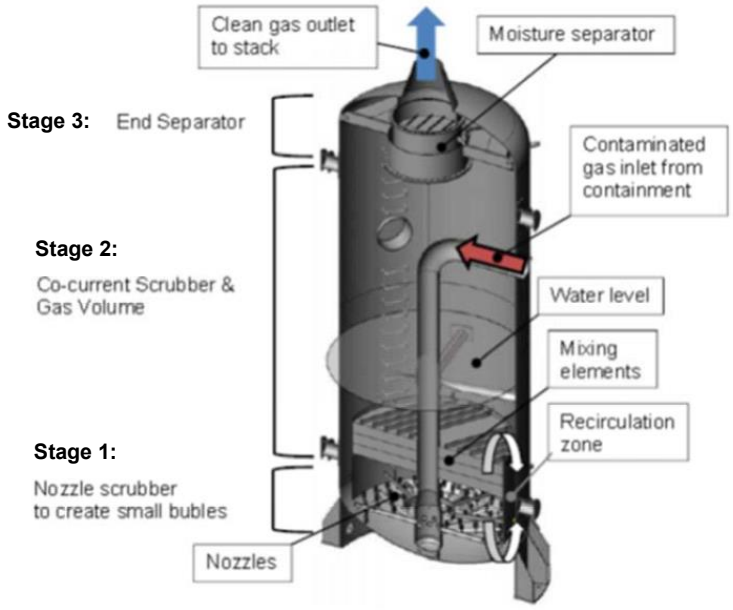

Figure 1. Schematic of the CCI-IMI-Nuclear Scrubber [1].

One of the outcomes of the study was the dependence of the DF on the flow regime and the residence time of the gas in the pool as shown in Figure 2. Despite the few data points and the fact that the regimes were determined by visual observations, the two flow regimes and a big decrease of the DF could be clearly distinguished. The authors of [7] postulated that the dependency of the retention must also come from the decrease of the interfacial area concentration coming from the different flow regimes since the residence time alone could not give a reasonable explanation. These results highlight the importance of a more detailed understanding the flow regime inside a wet scrubber under real conditions.

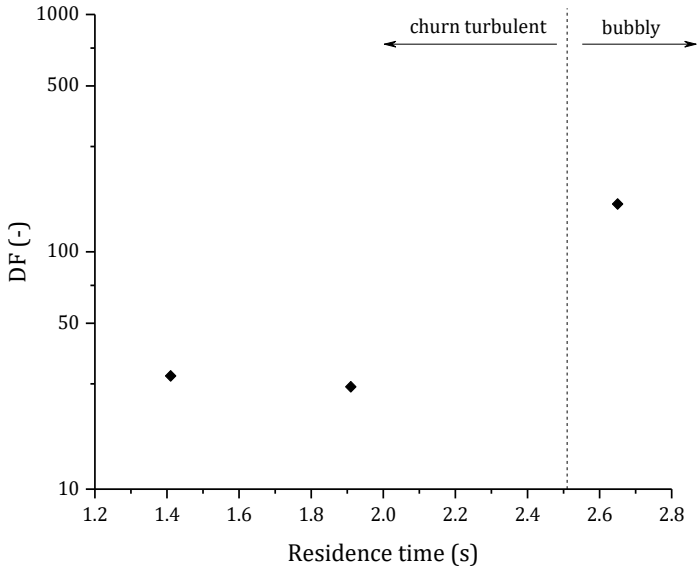

Figure 2. DF as a function of residence time showing significant change in the flow regime transition using the injector and mixing element from CCI-IMI-Nuclear and loaded with 0.06 M $Na_2S_2O_3$ and 0.1 M NaOH at 21 °C in the mini-VEFITA test facility [7].

The aim of this study was to make first attempts to characterize the flow regime for realistic inlet flow rates for the CCI injector with and without the mixing element using the wire-mesh sensor (WMS) technology. For the simplicity of the experiments, demineralized water was used inside the ISOLDE test facility with no addition of chemical scrubber solutions. The water temperature was set to ambient and the gas was dry nitrogen. Tests with steam in the carrier and gas at elevated temperatures are work in progress. The obtained data from the WMS are analyzed with published algorithms, i.e. bubble recognition and reconstruction [8], to determine the bubble size distributions and the interfacial area concentration of the flow. The hydrodynamic characteristics will be used in future work to improve the diffusion models for iodine retention with similar tests that have been conducted in mini-VEFITA with an iodine loaded gas.

2. EXPERIMENTAL SETUP

The requirements for the sensor equipment within mini-VEFITA to withstand the environment of the iodine chemistry were very high, e.g. the corrosiveness of iodine on steel or the high conductivity of the scrubber solutions. Therefore, the ISOLDE facility was built at PSI with the same geometry and dimensions as mini-VEFITA focusing on the instrumentation for bubble hydrodynamics. The facility has a modular design allowing to change the height by adding pipe modules as needed. The facility dimensions, i.e. an inner diameter of 0.2 m and 1.5 m height were maintained from mini-VEFITA. Additionally, more pipe compartments can be added to allow the injector nozzle to be moved by keeping the submergence level of the nozzle constant. This allowed the WMS to be flanged in the facility on a fixed position and thus made its design simpler. The wire-mesh sensor is installed after the glass pipe into the facility, as pictured in Figure 4.

2.1. Instrumentation

The WMS was chosen as the main measurement instrumentation for the characterization of the two-phase flow regime. The electrical scheme of the working principle is shown in Figure 3. This intrusive technique measures the electrical conductivity between two or three wire planes by applying a high frequent alternating voltage pulse on the transmitters and measuring simultaneously the incoming electrical current from the receiving layers. A more thorough description on the working principle of the WMS can be found in [9].
The conductivity data acquired by the WMS can be converted into void fraction information for each node $\varepsilon_{i,j,k}$ by using the calibration method presented in [10]. The conductance of each node $u_{i,j,k}$ is normalized with the liquid conductive value u_{liquid} to form the relative conductivity value $g_{i,j,k}$ as described in (1).

$$g_{i,j,k} = \frac{u_{i,j,k}}{u_{liquid}} \tag{1}$$

Maxwell's law can be applied in a second step which yields the gas fraction $\varepsilon_{i,j,k}$ as a function of the normalized conductivity $g_{i,j,k}$ as stated in (2) for each node in the sensor plane.

$$\varepsilon_{i,j,k} = \frac{1-g_{i,j,k}}{1+\frac{g_{i,j,k}}{2}} \tag{2}$$

The application of Maxwell's law promises a higher accuracy in detecting the bubble boundary than the previous linear interpolation as presented in (1) since it takes the disturbance of the potential field by the two-phase flow into account.

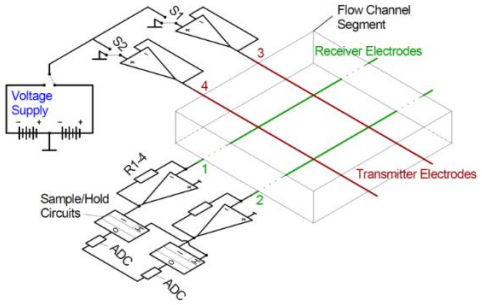

Figure 3. Electrical schematic of the wire-mesh sensor [10].

The sensor used in the ISOLDE facility consists of three layers holding 64 wires on each one of them. The pitch of the wires is 3 mm in lateral and 3.5 mm in axial direction. The stainless-steel wires have a diameter of 100 µm which is a compromise between reducing the intrusiveness of the sensor and the rigidity of the wires in the flow. The maximum measuring frequency is 2500 Hz. In the analysis of this work, the data from two layers are used to determine the bubble size distribution and interfacial area concentration. The third layer is installed for future work on the determination of the bubble velocity.

2.2. ISOLDE test facility

ISOLDE was designed as a versatile test facility for mid-scale two-phase flow measurements. By choosing out of the shelf equipment and building it at an elevated position, it allows for fast changes on the facility, e.g. exchange of the nozzle type or internals, depending on the focus of the work. The injector is fed by the nitrogen gas and steam supply and can be moved in vertical direction which enables measurements at

different positions in the flow by keeping the WMS at the same position. The additional facility length above the sensor allows to keep the submergence of the injector constant for each position. In Figure 4, the full height of the piping (3 m) is displayed. The installed sensor is visible at the first flange as indicated at a height of 1.5 m with the attached signal amplifiers and the data acquisition electronics.
The initial flow rates for the test matrix were chosen according to the conditions used in [7] to be able to compare the hydrodynamic data with the retention data from the mini-VEFITA facility. The submergence level of the injector was chosen to be 900 mm for these tests. The gas flow rates were increased, starting from 20 l_n/min up to 400 l_n/min as presented in Table I.

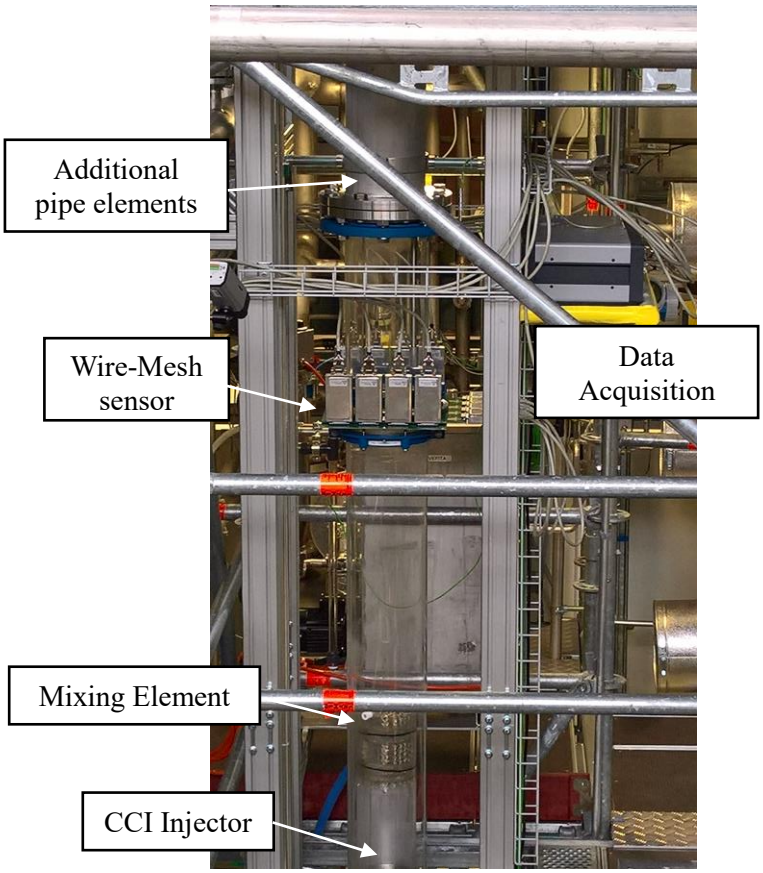

Figure 4. ISOLDE test facility with WMS data acquisition system, the CCI injector with mixing element and the additional pipe compartments on the top.

Table I. Gas flow rates for the tests performed at the ISOLDE facility

Test Conditions	Gas Injection Flow Rates [ln/min]									
With Mixing Element	20	-	50	-	-	100	150	200	300	400
Without Mixing Element	20	40	-	60	80	100	-	200	300	400

For the tests with the mixing element, the WMS was positioned approximately 50 mm below the water surface, resulting in 842 mm distance. Unfortunately, the physical presence of the mixing element made measurements at closer positions to the injector impossible. In the test cases without the mixing element, the nozzle was placed closer to the WMS with a distance of 722 mm to avoid distortions coming from the pool surface. In both cases, the flow was fully developed. The temperature of the injected nitrogen gas and the water column was kept at ambient temperature of 25 °C to neglect in these first tests the effects of

temperature. A small amount of sodium sulfate was added to the demineralized water to increase the electrical conductivity into the lower working range of the WMS without affecting the surface tension of water [12]. The concentrations were around 0.04 g/L for the experiments with the mixing element and around 0.046 g/L for the ones without.

3. METHODOLOGY

The bubble recognition algorithm starts to assign bubble ID numbers starting from a threshold of 10%. The noise signal in the data is causing bubbles to artificially being unified or noise elements being recognized as bubbles. The low electrical conductivity of the demineralized water requires a high amplification of the incoming signal which also amplified the overlaying noise signal. A filter had to be applied to reduce the noise in the signal. According to previous experience with the WMS, the void gradient at the edge of a bubble is usually higher than the amplitude of the noise signal. A simple algorithm was designed to be used on the raw data that compared the difference of the void with the six Von Neumann neighbors of all data points with a void value of less than 5 %. This threshold was chosen by studying the standard deviation of the noise signal in the raw data. If one of the six differential values showed a void difference higher than 10 %, the value was retained, as it would correspond to the bubble boundary. Otherwise, the value would be set to 0 % void.
The high bubble density of the bubble swarm added as well to the difficulty of the analysis. The data was analyzed in a further step using a higher threshold of 10 % for triggering the filter and 20 % void difference as a criterion to keep the data point. The results of this adjustment did not affect the results too strongly which led to the decision to keep the filtering threshold rather low to keep the manipulation of the filter on the data points as limited as possible.
After the bubble recognition, further analysis was carried out to calculate the bubble interfacial area and the volume of each bubble [8], [13]. A flood fill algorithm recognizes common void areas via the Von Neumann neighbors up to a dynamically set threshold and a linear interpolation scheme determines the volume and surface of each bubble. The equivalent bubble diameter d_{eq} is calculated by the bubble surface A and the bubble volume V, assuming spherical bubbles as shown in (3).

$$d_{eq} = \sqrt[3]{\frac{6\,V}{\pi}} \tag{3}$$

4. RESULTS AND DISCUSSION

In a first step, the flow regimes for the different gas inlet flow rates had to be characterized. Two regimes were mainly observed in [7], homogeneous bubbly flow for all flow rates below 200 l_n/min and heterogeneous bubbly and churn turbulent flow for higher flow rates. In ISOLDE, the water was not loaded with any chemicals which makes the obtained results quantitatively not comparable. However, qualitative comparisons are applicable to the tests performed in mini-VEEFITA. To quantify the flow field, the volumetric probability share was calculated based on the WMS data acquired at the ISOLDE facility. The estimation of the uncertainty is still undergoing work and needs more validation data. The progression of the noise signal on the determination of the bubble size is unfortunately not very straight forward.
In Figure 5, the volumetric share over the equivalent bubble diameter is displayed. The volumetric share represents the relative amount of gas volume covered by bubbles of that particular size to the total gas volume. It shows that the assumption for bubbly flow holds for 20 l_n/min until 50 l_n/min where small bubbles around 1 mm diameter contribute the most to the volume. From 100 l_n/min onwards, the distribution changes its shape into a bimodal curve indicating the formation of bigger caps and churns. The visualization of the raw data revealed that already at comparably small flow rates, caps are formed in the center of the pipe that are covered by the bubble swarm close to the wall and thus not visible to the eye. With an increasing flow rate, the volumetric contribution of the small bubbles decreases, and the equivalent bubble diameter of the churns is increasing, i.e. the churns grow in volume.

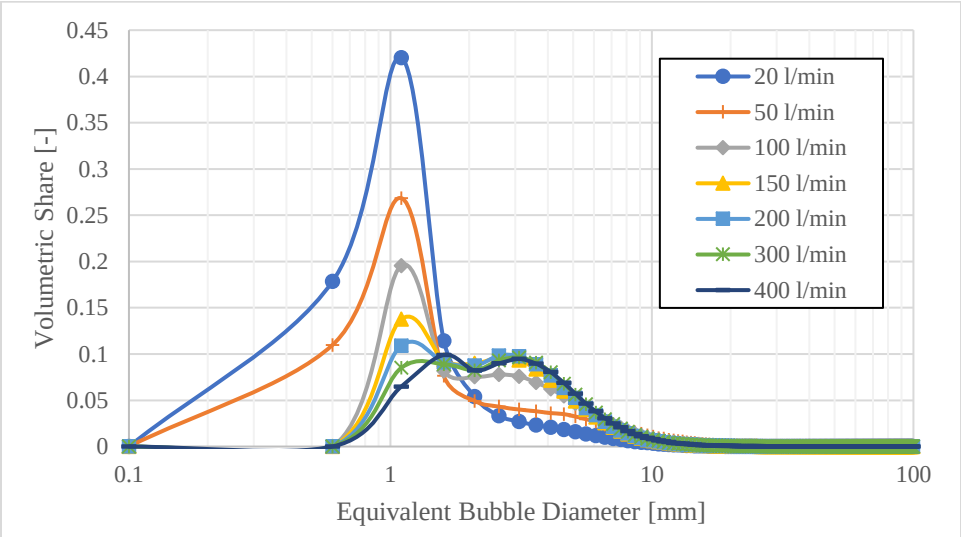

Figure 5. Volumetric share of the bubbles in dependence of the equivalent bubble diameter at a distance of 842 mm from the CCI injector with the mixing element for different flow rates at adiabatic temperature conditions.

The results of the data without the mixing element show a different picture. As illustrated in Figure 6, the flow is not deviating from its unimodal distribution. The peak of the most bubbles is at the same bubble size but with at a smaller share than with the mixing element. The mixing element seems to work well in breaking up bubbles into less than 1 mm bubbles for flow rates less than 100 l_n/min. Above 100 l_n/min, the peak of the distribution starts to move towards bigger diameter and the distribution becomes flatter towards bigger diameters which corresponds to a more heterogeneous flow. In the same range above 100 l_n/min, the mixing element is keeping the peak at roughly 1 mm diameter bubbles and causing a more distinct heterogeneous flow between the two types of bubble sizes.

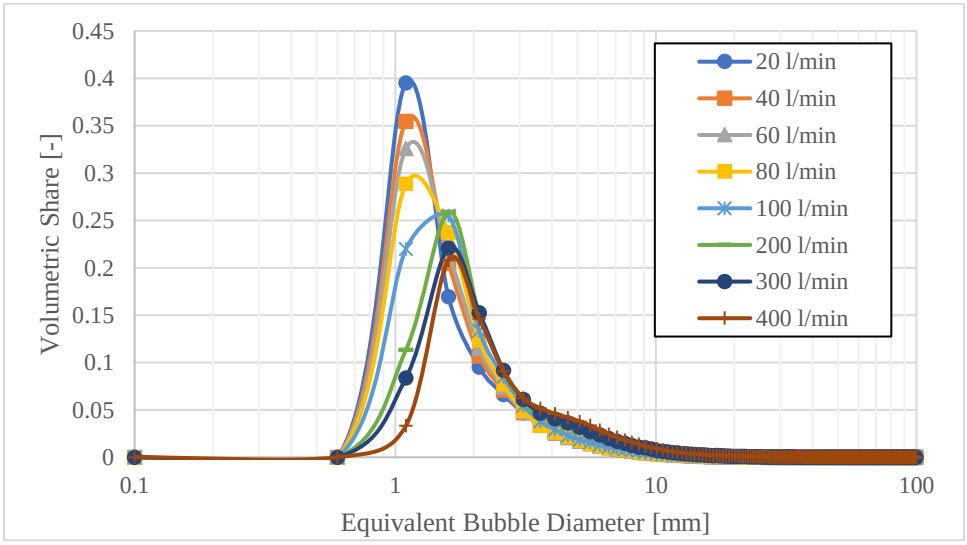

Figure 6. Volumetric share of the bubbles in dependence of the equivalent bubble diameter at a distance of 722 mm from the CCI nozzle without the mixing element for different flow rates at adiabatic temperature conditions.

The turning point from bubbly flow to churn-turbulent flow was found to be much later in the work of [7] but there the surface tension was lowered by the sodium sulfate and the sodium hydroxide which were added in the scrubber solution to retain iodine, causing furthermore foam formation and higher swell levels. Still, as mentioned before, the first churns form in the center of the pipe which might not have been detected by the visual observations of [7]. The work of [15] summarized the dependency of the flow regime on the superficial velocity and the bubble column diameter under the influence of various sparger diameters and dilutes. According to [15], the transition regime from bubbly flow to churn-turbulent for a bubble column of a diameter of 0.2 m can be roughly approximated in the range from 0.04 m/s to 0.07 m/s superficial gas velocity as shown in Figure 7, depending on the liquid and the orifice diameter of the nozzle. This superficial velocity corresponds in the case of ISOLDE to 75 – 130 l_n/min. The results obtained from the bubble size distributions in Figure 5 and Figure 6 are in very good agreement with the proposed regime transition of [15], showing a change of the distribution shape around 100 l_n/min for both cases.

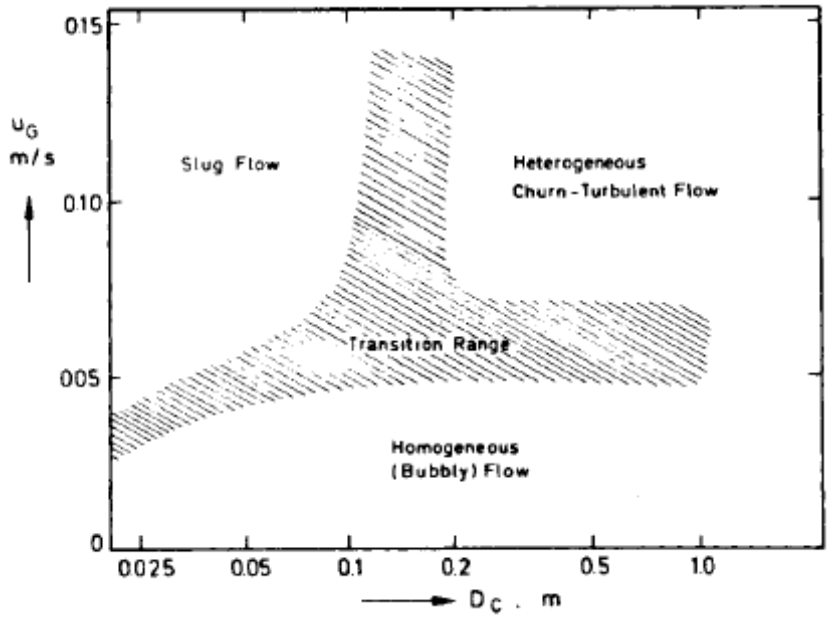

Figure 7. Approximate dependence of flow regime on gas velocity and column diameter (water and dilute aqueous solutions) [15].

The average void fraction in Figure 8 also confirms the transition range that was found in [15]. The slope of the curve is changing for both cases around the postulated superficial velocities as highlighted in Figure 8 which is to be expected in case of a regime change. For higher flow rates above 300 l_n/min, the void fraction seems to converge towards the same average void value.

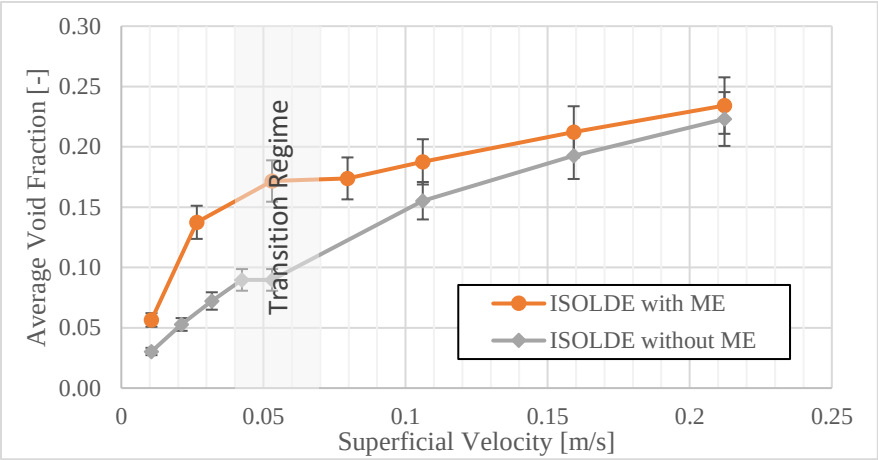

Figure 8. Evolution of average void fraction for different gas flow rates compared and the distinction between bubbly and churn-turbulent flow at adiabatic temperature.

Besides the bubble size distributions and the void data, the acquired data from the WMS allow the determination of the interfacial area concentration inside the test facility. The results in Figure 9 show that the interfacial area concentration is significantly higher with the mixing element than without it. This was to be expected since the smaller bubbles that are created by the bubble breaker contribute with a higher interface to volume ratio. However, the trend is similar in both cases showing an increase with superficial velocity in the bubbly flow regime and a decrease when transiting into the churn-turbulent regime. This decrease should also have an impact on the mass transfer since less interface is available for scrubbing. It would also be in compliance with the assumptions made in [7].
The interfacial area peaks around the transition regime of the flow as indicated in Figure 9 which follows the estimated flow regimes and the results gained so far. As seen before in the bubble size distributions, the churns grow in volume size as well as in their volumetric share. The interfacial area of this churns on the other hand seems to grow significantly slower, which leads to a decrease of the interfacial area concentration.

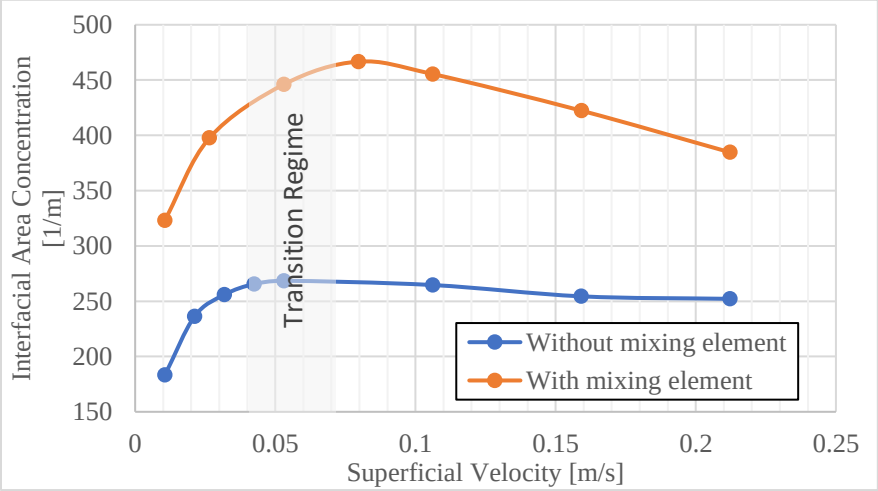

Figure 9. Interfacial area concentration for different flow rates with the CCI injector with and without mixing element at adiabatic temperature conditions.

The evolution of the interfacial area density emphasizes again the importance of the hydrodynamics for wet scrubbers. So as the authors of [7] assumed, the lower decontamination factor in Figure 2 can most probably also be linked to the decrease of the interfacial area. The data obtained from mini-VEFITA with iodine loaded feeding gas in pure water under the same conditions as in ISOLDE will show if the assumptions made from these hydrodynamic tests hold true for the scrubbing efficiency of the bubble column.

5. CONCLUSION

The test facility ISOLDE has been built to investigate the hydrodynamic characteristics of two-phase flow regimes. First tests have been done to get an insight into the flow regime in wet scrubbers for two different cases. A CCI nozzle with a Sulzer Chemtech mixing element was used for the first test case. In the second one, the mixing element was removed to quantify the effect of the bubble breakup. The wire-mesh sensor technique was chosen as the main instrumentation to characterize the flow.
The gas injection flow rate was varied for both test cases to get an idea of the flow conditions inside the bubble column. The results coming from the bubble size distributions revealed the transition of the flow regime to lie within the expected range coming from literature [15] where the transition regime from bubbly to churn-turbulent would be estimated at similar flow conditions, i.e. 75 – 130 l_n/min for a bubble column of 200 mm diameter. In terms of interfacial area concentration, the maximum was reached at flow rates around the same mentioned transition regime. The optimal working range to increase the interfacial area to a maximum for the mixing element in pure water was found to be around 100 - 150 ln/min. In both test cases, the interfacial area concentration would drop from there onwards for all higher injection flow rates. The interfacial area concentration seems to play a role in terms of scrubbing efficiency, but further research will be necessary to find its place among the hydrodynamic parameters that are affecting the mass transfer. Furthermore, more measurements need to be conducted at different measurement positions to deepen the understanding of the different stages of the flow regime. Additionally, new experiments with the commercial chemical scrubbing solution as well as elevated temperatures, different injection nozzle geometries and sizes are necessary to replicate more realistic wet scrubber operation conditions. The effect of the chemicals on the surface tension and therefore on the bubble sizes cannot be neglected. The WMS will need some improvements and upgrades to be able to work in this high conducting scrubbing solutions.

ACKNOWLEDGMENTS

This work was partially funded by Swissnuclear, the association of the Swiss nuclear power station operators. Part of the studies also received funding from the Horizon 2020 research program from the European Union under the Marie Sklodowska-Ourie grant agreement No. 701647. Many thanks go also to Hauke Schütt from PSI who supported us during the whole built-up phase and the endless hours of debugging the controls of the ISOLDE facility.

REFERENCES

1. D. Jacquemain, S. Guentay, S. Basu, M. Sonnenkalb, L. Lebel, H.J.Allelein, B. Liebana Martinez, B. Eckhardt, L. Ammirabile, “OECD/NEA/CSNI Status Report on Filtered Containment Venting”, NEA/CSNI/R(2014)7, July 2014, Nuclear Energy Agency.
2. M. Ali, C. Yan, Z. Sun, H. Gu, J. Wang, K. Mehboob, “Iodine removal efficiency in non-submerged and submerged self-priming venturi scrubber”, *Nuclear Engineering and Technology*, **45(2)**, pp. 203–210 (2013).
3. M. Ali, C. Yan, Z. Sun, H. Gu, J. Wang, “Study of iodine removal efficiency in self-priming venturi scrubber”, *Annals of Nuclear Engineering,* **57**, pp. 263–268 (2013).

4. N.P. Gulhane, A.D. Landge, D.S. Shukla, S.S. Kale, "Experimental study of iodine removal efficiency in self-priming venturi scrubber", *Annals of Nuclear Energy*, **78**, pp. 152–159 (2015).
5. Y. Zhou, Z. Sun, H. Gu, Z. Miao, "Performance of iodide vapour absorption in the venturi scrubber working in self-priming mode", *Annals of Nuclear Energy*, **87**, pp. 426–434 (2016).
6. P. Goel, A. Moharana, A.K. Nayak, "Measurement of scrubbing behaviour of simulated radionuclide in a submerged venturi scrubber", *Nuclear Engineering and Design*, **327**, pp. 92–99 (2018).
7. I. Beghi, T. Lind, H.-M. Prasser, "Experimental studies on retention of iodine in a wet scrubber", *Nuclear Engineering and Design*, **326**, pp. 234–243 (2018).
8. H.-M. Prasser, D. Scholz, C. Zippe, "Bubble size measurement using wire-mesh sensors", *Flow Measurement and Instrumentation*, **12**, pp. 299–312 (2001).
9. H.-M. Prasser, A. Böttger, J. Zschau, "A new electrode-mesh tomograph for gas-liquid flows", *Flow Measurement and Instrumentation*, **9**, pp. 111–119 (1998).
10. T. T. Betschart, "Two-Phase Flow Investigations in Large Diameter Channels and Tube Bundles", Doctoral Thesis, DISS. ETH No. 22954 (2015).
11. H.-M. Prasser, R. Häfeli, „Signal response of wire-mesh sensors to an idealized bubbly flow", *Nuclear Engineering and Design*, **336**, pp. 3–14 (2018).
12. A. P. dos Santos, A. Diehl, Y. Levin, „Surface Tensions, Surface Potentials, and the Hofmeister Series of Electrolyte Solutions, *Langmuir*, **26 (13)**, pp. 10778–10783 (2010).
13. H.-M. Prasser, "Evolution of interfacial area concentration in a vertical air-water flow measured by wire-mesh sensors", *Nuclear Engineering and Design*, **237**, pp. 1608–1617 (2007).
14. D. Ito, H.-M. Prasser, H. Kikura, M. Aritomi, "Uncertainty and intrusiveness of three-layer wire-mesh sensor", *Flow Measurement and Instrumentation*, **22**, pp. 249–256 (2011).
15. Y. T. Shah, B. G. Kelkar, S. P. Godbole, W.-D. Deckwer, "Design Parameters Estimations for Bubble Column Reactors", AlChE Journal, **28 (3)**, pp. 353–379 (1982).